www.serd.ait.ac.th/reric

Computational Investigation of Energy Efficient Pin Fin Cross Section for a Compact Heat Exchanger

I. Khan*, M. Baruah*, A. Dewan+1 and P. Mahanta*

Abstract – *This paper presents the computational investigation of compact heat exchangers that are primarily used in dissipating heat generated by electrical and/or electronic components and assemblies. In order to assess the effect of pin cross-section on the pressure drop and heat transfer capabilities, six different types of pin cross sections, namely, elliptical, straight circular, 2° tapered circular, 4° tapered circular, drop and hexagonal, were computationally investigated. The heat exchanger channel is characterized by the presence of the fins mounted vertically on a horizontal base plate in a staggered arrangement along the flow direction. Aluminum was considered to be the material of pin fins. The fluid flow inside the heat exchanger channels is assumed to be three-dimensional, incompressible and steady. Pressure, temperature and velocity profiles at different locations within the computational domain are considered for different Reynolds number. The thermal and fluid dynamic characteristics of six pin fin heat exchangers along the computational domain are discussed in detail. We have shown that a small amount of tapering significantly improves the performance of heat exchanger. The results show that the overall performance of elliptical pin fins is better than other pin cross sections considered. This makes the elliptical fin arrays a promising cooling device for high thermal loaded electronic components.*

Keywords – CFD, heat transfer, performance comparison, pin fins, pressure drop, and turbulence.

1. INTRODUCTION

The primary goal of a heat exchanger design is the acquirement of high thermal performance. For this, various techniques have been developed by many researchers during last few decades. Among them, staggered finned ducts are one of the widely used passive methods for the enhancement of heat transfer. These are commonly used in compact heat exchangers to reduce the size of heat exchanger. Generally, attached fins in channel play the role of extension of the heat transfer area, while they also lead to the pressure loss. Therefore, heat exchangers should be designed by considering both the pressure loss and the heat transfer. With an increase in circuit density and power dissipation of integrated circuit chips and other microelectronics devices, there is a need for employing effective cooling devices and cooling methods to maintain the operating temperatures of electronics components at a safe and satisfactory level. The heat sink industry, traditionally the supplier of cooling products, is always searching for new technologies which enhance thermal performance with minimum penalty, i.e., pumping power. For this reason, a comparison in geometry of pin fin heat sinks is of interest and needs to be investigated to determine applicability as a general cooling product. During the last few decades, many researches have been conducted on predicting the flow and thermal characteristics in various different types of heat exchangers for optimal design. One of the most common designs in these applications employ an enclosed pin fin heat exchanger duct flow configuration with pins of circular cross-section. Other pin fin shapes have received limited attention. Round pin fins have the disadvantage of early flow separation over the fin, which lowers the heat transfer and increases the total pressure drop across the heat exchanger. When looking to improve the performance of these heat exchangers, one particular area of interest lies in using different pin shapes that are able to delay the flow separation. A thorough experimental characterization of different possible shapes is an expensive and time consuming task, due to the enormous cost of experimental parts and tools. In addition, there is little geometric flexibility built into test models, and a new model has to be constructed for each different configuration.

A computational study can offer a remedy for this problem by offering a quick and cost effective means of study with the advantage of having large flexibility in the geometry and boundary conditions. Many configurations can be studied at different Reynolds numbers and turbulence levels, and many different pin shapes and arrangements can be investigated. After selecting an optimum heat exchanger design based on numerical study, an experiment can be conducted on a far narrower range of options to validate the predicted performance of the heat exchanger design.

Over the last couple of decades a large number of researches have been performed to study the pressure drop and heat transfer characteristics of compact heat exchangers. Kays [1] presented experimental data for four in-line pin arrangements and one staggered arrangement of pin fins as elements for heat transfer

*Department of Mechanical Engineering, Indian Institute of Technology Guwahati, Guwahati – 781039, India.

+Department of Applied Mechanics, Indian Institute of Technology Delhi, Hauz Khas, New Delhi – 110016, India.

[1]Corresponding author; Tel: + 911126591971 Fax: + 911126581119
E-mail: adewan@am.iitd.ac.in.

enhancement. It was demonstrated that owing to a high area to perimeter ratio, pin fins provide a method for obtaining very high heat transfer coefficients while at the same time maintaining high fin effectiveness. He concluded that despite high friction factors of pin fin surfaces, it is possible to design heat exchangers that are competitive, from volume and weight points of view, with heat exchangers having continuous or louvered fins. Basic research on heat transfer and pressure drop characteristics was performed by Theoclitus [2] who performed a limited parametric study of pin fins with an in-line arrangement. Sparrow *et al.* [3] reported an excellent experimental work on the influence of tip clearance for a staggered wall-attached array of cylinders. They obtained data on heat transfer coefficients by applying the analogy between heat and mass transfers via the naphthalene sublimation technique. They found that the heat transfer coefficient increases moderately as the length of the cylinder increases and the tip clearance between the pin and the shroud decreases. On the other hand, the array pressure drop increases markedly with increasing cylinder length.

Ota *et al.* [4] studied the heat transfer and flow around an elliptic cylinder of axis ratio 1:3. Their experimental results showed that heat transfer coefficient of the elliptic cylinder is higher than that of a circular one with equal circumference and the pressure drag coefficient of the former are much lower than that of the latter. Lee [5] presented an analytical procedure for selecting optimum heat sinks based on the simulation results and illustrated the effect of various design parameters on the performance of heat sinks. The influences of the pin fin distance and the pin fin material on the thermal performance of the inline and staggered pin fin assemblies were studied experimentally by Haq *et al.* [6]. They determined the optimal fin distance in the streamwise direction for a uniform spanwise distance and noted that the optimal spacing increases as the thermal conductivity of the pin fin material increases. Further, they noted that the overall pressure drop for all tested configurations increases steadily with increasing mean inlet velocity and with decreasing uniform pin fin spacing.

Chen *et al.* [7] conducted similar experiments with drop-shaped pin fins, again using the concept of equal circumference diameter. They also found much less pressure loss levels for drop shaped pin fins, but similar to those observed by Li *et al.* [8]. This was mainly due to the smaller frontal area of the drop-shaped fins in order to achieve the same surface area with the corresponding circular fins. They showed that the heat transfer levels of drop-shaped pin fin arrays were higher than the levels for circular pin fin arrays. Experiments were carried by Li *et al.* [8] to investigate the heat transfer and flow resistance characteristics in rectangular ducts with staggered arrays of short elliptic pin fins in a cross flow of air. The major and minor axes of the elliptical fins were chosen such that their circumference is equal to the circumference of a corresponding circular pin fin. The experimental results showed that the heat transfer of a channel with elliptic pin fins is somewhat higher than that with circular pin fins while the resistance of the former is much lower than that of the latter in the Reynolds number range from 1,000 to 10,000.

Behnia *et al.* [9] attempted to compare the heat transfer performance of various commonly used fin geometries. The basis of comparison was chosen to be a circular array of 1.0 mm diameter pin fins with a 2.0 mm pitch. The pitch to width ratios of the other geometries were chosen to provide equal ratios of fin area to base area. In all cases, staggered geometries performed better than inline configurations. At lower values of the pressure drop and pumping power, elliptical fins worked best. At higher values, round pin fins offered the highest performance. Experiments were carried by Uzol *et al.* [10] for investigation of the wall heat transfer enhancement and total pressure loss characteristics for two alternative elliptical pin fin arrays and the results were compared with the conventional circular pin fin arrays for a range of Reynolds numbers from 10,000 to 47,000. The results show that on an average the wall heat transfer enhancement capability of the circular pin fin array is about 25-30% higher than that of the elliptical pin fin arrays. However in terms of the total pressure loss, the circular pin fin arrays cause 100-200% more pressure loss than that for the elliptical pin fin arrays. Moshfegh and Nyiredy [11] compared five different turbulence models for pin fin heat sinks, namely, the standard k-ε model, RNG k-ε model, the realizable k-ε model, the k-ω model, and the Reynolds stress transport model. Dewan *et al.* [12] presented an overview of different methods proposed in the literature for heat transfer augmentation. Sahiti *et al.* [13] numerically examined six pin shapes, namely NACA, dropform, lancet, elliptic, circular, and square by assuming the flow to be laminar. Their simulations showed that NACA profile offers little advantage. Encompassing the constraints of the same hydraulic diameter, coverage ratio, and pin length, they showed that circular pin fin having inline arrangement outperform other configurations.

Yang *et al.* [14] performed an experimental study of pin fin heat sinks having circular, elliptic, and square cross-sections. A total of twelve pin fin heat sinks with inline and staggered arrangements were made and tested. The effect of fin density on the heat transfer performance was examined. For an inline arrangement, the circular pin fin shows an appreciable influence of fin density whereas no effect of fin density is seen for square fin geometry. This is associated with the unique deflection flow pattern accompanied with the inline circular fin configuration. For the staggered arrangement, the heat transfer coefficient increases with a rise of fin density for all the three configurations. The elliptic pin fin shows the lowest pressure drops. For the same surface area at a fixed pumping power, the elliptic pin fin possesses the smallest thermal resistance for the staggered arrangement.

Based on the literature survey it can be concluded that a single comparative study dealing with important geometries of pin fin cross section with a detailed

investigation under turbulent flow conditions has not been reported in the literature. The heat transfer behavior can change significantly if the realistic situation of turbulence in the pin fin heat exchanger is considered. The objective of the present work is to investigate the different pin fin cross-section in a rectangular channel with staggered fin arrays and characterize the heat transfer and associated pressure drop behavior using the RNG *k-ε* model. The computational domain is assumed to be three-dimensional, periodic, and flow is considered to be turbulent. For an easy comparison of the heat sink geometries, equal wetted surface area of the fins is considered.

2. GEOMETRY AND FLOW DESCRIPTION

Pin-fin arrangement

Two types of arrangements are most commonly used in practical applications: staggered and inline (Figure 1). Sahiti *et al.* [13] showed that the staggered arrangement provides more heat transfer rate than the inline arrangement for different fin cross sections, and therefore the staggered arrangement is considered in the present work.

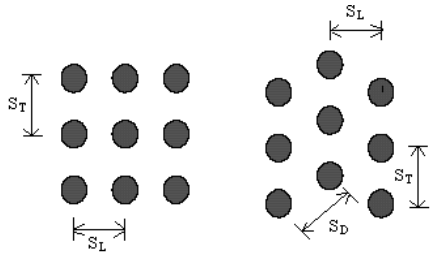

Fig.1. (a) Inline arrangement and (b) staggered arrangement.

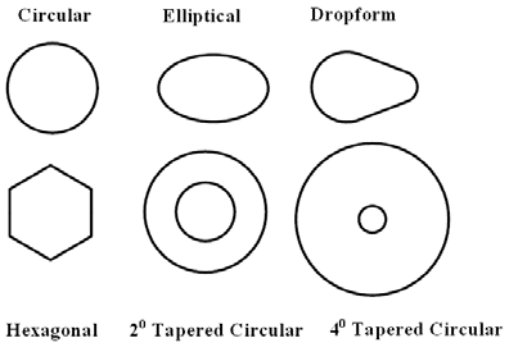

Fig. 2. Cross-sections of selected pin fins geometries.

The flow in a staggered arrangement is characterized by a periodic separation and joining of fluid streams whereas in an inline arrangement, the flow resembles a flow through a channel with wavy side walls. Thereby a large part of the fluid bypasses the fins. This results in a lower increase of fluid temperature. Hence the heat transfer in an inline arrangement is less than that in the staggered arrangement. A schematic of the pin fin heat sink model used in the present study is shown in Figure 3.

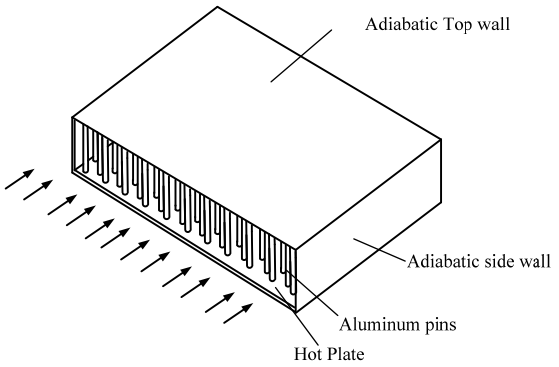

Fig. 3. Pin fin heat sink model.

3. COMPUTATIONAL DOMAIN AND GOVERNING EQUATIONS

Computational domain

Flow over tube banks with more than sixteen rows is considered to be fully developed, where there is no change in the flow and temperature. Thus heat transfer and pressure drop characteristics derived from the array of sixteen rows are valid also for pin fin arrays with a large number of pins in the flow direction. Therefore the computational domain in the present work consists of sixteen rows of pin fins in the flow direction for all six forms of pin fins compact heat exchangers. Aluminum is considered to be the material of pin fins.

The computational domain used in the present work for circular pin fins as shown in Figure 4 has a width a = 3.60 mm, length L = 155.31 mm and fin height h = 23.0 mm. The diameter of the fins d = 2.3 mm. Two symmetry planes are passed through the middle of the fins of two consecutive rows. The computational domain for others pin fin cross sections are exactly the same as that for circular pin fins. The circular pin fins are replaced by others pin fins whose dimensions are shown in Figure 5. The heights of all the pin fins considered are 23.0 mm. The position of the centre of gravity for the rest of the pin fins is same as circular pin fins. The total surface area of different pin fins considered for convection heat transfer was also the same for all the cases. The hydraulic diameter for the flow domain is calculated from the expression $D_h = (4*A_c*L) / A_{t,}$ (where A_c denotes the minimum heat exchanger flow area, L the length of the fins, A_t the total heat transfer area). D_h depends on pin fin cross section. It may be noted that value of D_h = 2.0 mm considered in the present study is widely used for the cooling of electronic appliances using pin fin heat exchangers. The pins, which are considered as solid are placed in the computational domain and surrounded by the fluid. The length of the flow developing inlet block was taken to be $5D_h$ whereas the outlet block length was set equal to $15D_h$ in order to avoid any influence of the eventual back flow streams on the final results. The volume of the computational domain considered was the same for all the geometries.

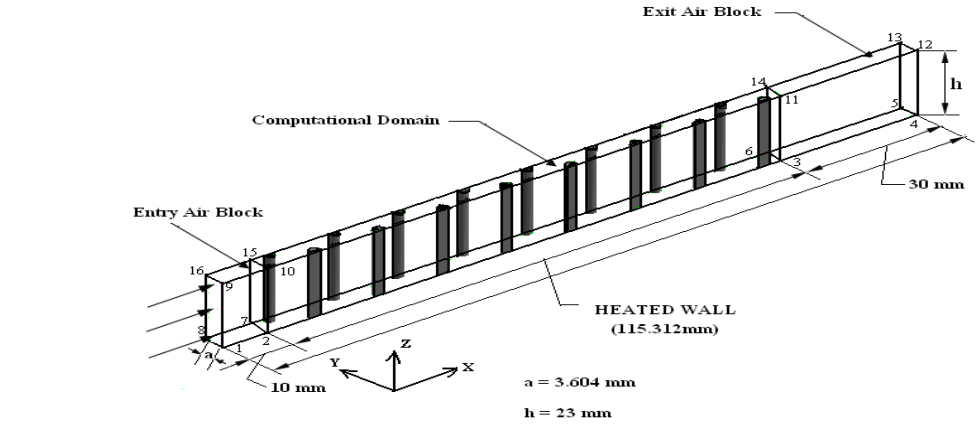

(a)

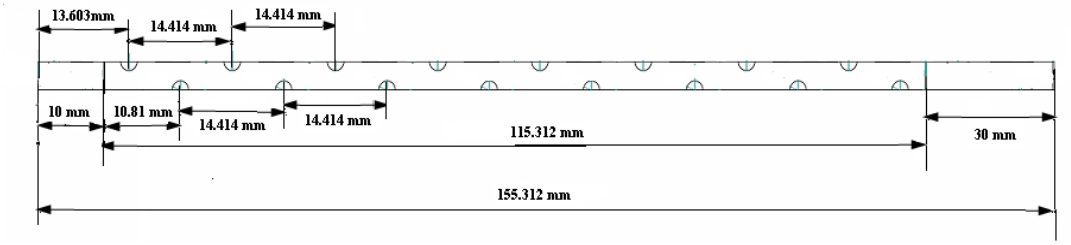

(b)

Fig. 4. Computational domain for circular pin fins.

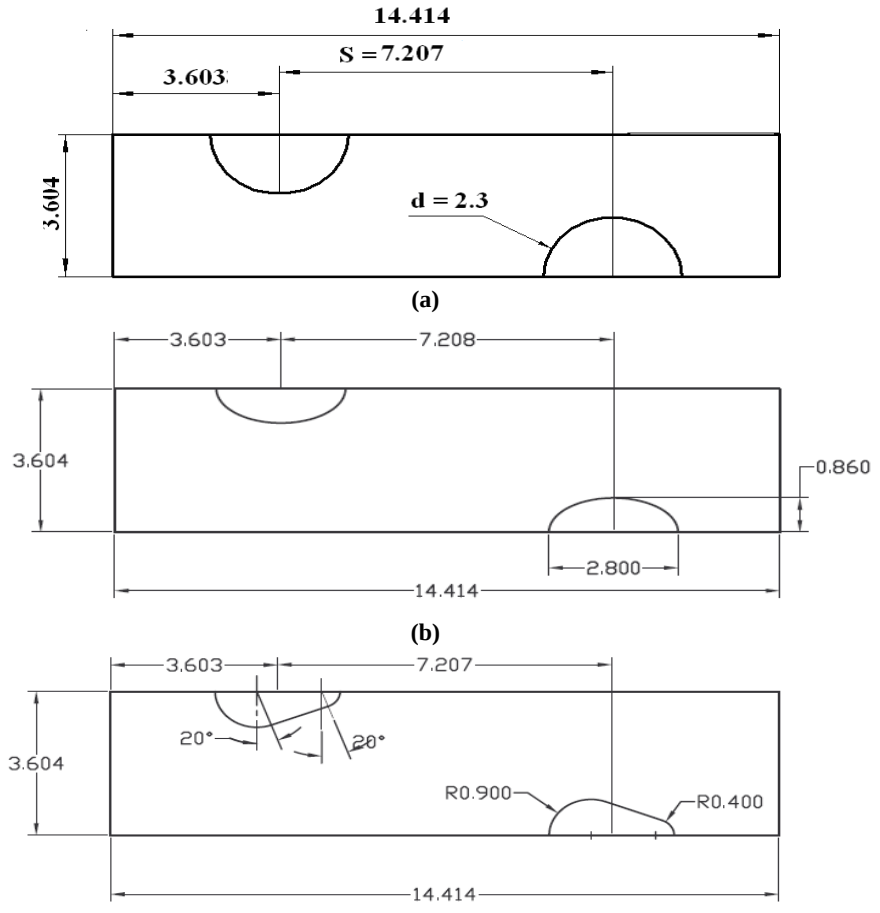

(a)

(b)

(c)

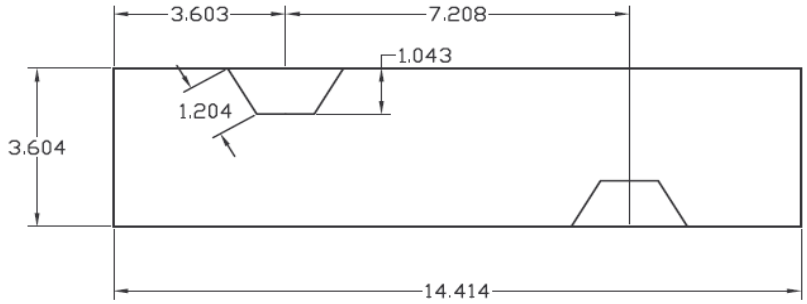

(d)

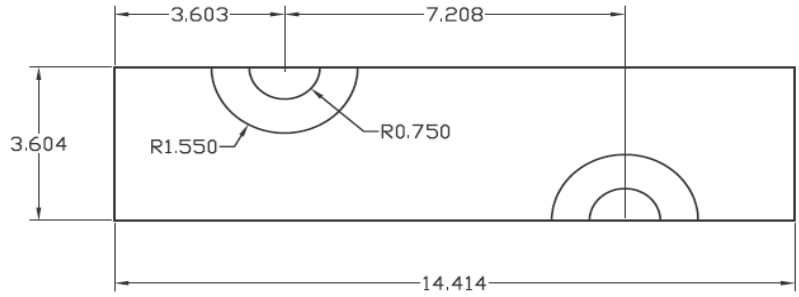

(e)

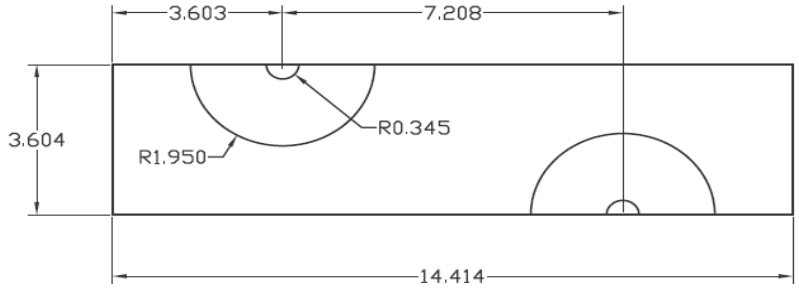

(f)

Fig. 5. Dimensions in mm of unit cells (a) straight circular pin fin, (b) elliptical pin fin, (c) drop pin fin, (d) hexagonal pin fin, (e) 2º tapered circular pin fin and (f) 4º tapered circular pin fin.

Governing equations

The flow in the heat exchanger was assumed to be steady and incompressible. The governing continuity and momentum equations neglecting body forces can be written in the Cartesian tensor form as [15]:

$$\frac{\partial(\rho u_i)}{\partial x_i} = 0 \tag{1}$$

$$\rho u_i \frac{\partial u_j}{\partial x_i} = -\frac{\partial p}{\partial x_j} - \frac{\partial \tau_{ij}}{\partial x_i} \tag{2}$$

where for Newtonian fluids, the molecular dependent momentum transport term is given by:

$$\tau_{ij} = -\mu_t \left(\frac{\partial u_i}{\partial x_j} + \frac{\partial u_j}{\partial x_i} \right) + \frac{2}{3}\delta_{ij} k \tag{3}$$

where i, j = 1, 2, and 3. The governing equation for solving the temperature field is provided by:

$$\rho c_p u_i \frac{\partial T}{\partial x_i} = k_f \frac{\partial^2 T}{\partial x_i^2} - \frac{\partial}{\partial x_i}(\rho c_p \overline{u_i' T'}) \tag{4}$$

where u_i denotes the velocity components in the Cartesian coordinate system with its coordinates x_i, T the fluid temperature, p the pressure and k_f the thermal conductivity of the fluid.

The conjugate heat transfer from pin fin arrays implies the simultaneous solution of Equations 1 to 4 and the energy equation in the solid, which reads:

$$\frac{\partial^2 T_s}{\partial x_i^2} = 0 \tag{5}$$

The transport equations for turbulence kinetic energy (k) and its rate of dissipation (ε) according to the RNG k-ε model [16] are given as:

$$\frac{\partial}{\partial t}(\rho k) + \frac{\partial}{\partial x_i}(\rho k u_i) = \frac{\partial}{\partial x_j}\left(\frac{\mu_{eff}}{\sigma_k} \frac{\partial k}{\partial x_j} \right) + G_k - \rho\varepsilon \tag{6}$$

$$\frac{\partial}{\partial t}(\rho\varepsilon)+\frac{\partial}{\partial x_i}(\rho\varepsilon u_i)=\frac{\partial}{\partial x_j}\left(\frac{\mu_{eff}}{\sigma_\varepsilon}\frac{\partial\varepsilon}{\partial x_j}\right)$$

$$+C_{1\varepsilon}\frac{\varepsilon}{k}G_k-C_{2\epsilon}\rho\frac{\varepsilon^2}{k}-R_\varepsilon \quad (7)$$

$$R_\varepsilon=\frac{c_\mu\rho\eta^3(1-\eta/\eta_0)}{1+\beta\eta^3}\frac{\varepsilon^2}{k}\quad \eta=S\frac{k}{\varepsilon} \quad (8)$$

The model constants are $C_\mu = 0.0845$,

$C_{1\varepsilon}=1.42, C_{2\varepsilon}=1.68, \sigma_k=\sigma_\varepsilon=0.7178, \beta=0.012$.

Turbulent heat fluxes in the thermal energy equation are modeled as

$$-\rho\overline{u_i'T'}=-\frac{\mu_t}{\mathrm{Pr}_t}\frac{\partial T}{dx_i} \quad (9)$$

The eddy viscosity is computed as:

$$\mu_t=\rho C_\mu k^2/\varepsilon \quad (10)$$

The standard law of the wall for velocity was used. The law of the wall for temperature used in the present work is of the form [17]:

$$T^+=\mathrm{Pr}\,[\ln(EY^+)+P] \quad (11)$$

$$P=9.24\{(\mathrm{Pr}/\mathrm{Pr}_t)^{3/2}-1\}[1.28\,e^{-0.007\mathrm{Pr}/\mathrm{Prt}}] \quad (12)$$

Here Pr_t denotes the turbulent Prandtl number and is taken as 0.85 and Pr = 0.71 for air. The physical properties of air considered are ρ = 1.225 kg.m^{-3}, μ = 1.789x10^{-5} kg. (ms)$^{-1}$ and C_p = 1006.43 Jkg^{-1} K^{-1}.

4. ASSUMPTIONS AND BOUNDARY CONDITIONS

Assumptions

Due to the complexity of the flow around a single cylinder or a cylindrical pin in a pin-fin heat sink, it is necessary to make some assumptions to simplify the analysis. The assumptions made in the present study are:

1. The fin tips are adiabatic.
2. There is no airflow bypass, i.e., the heat sink is fully ducted.
3. The approaching airflow is normal to the pin-axis.
4. The approach velocity is uniform for each row in a heat sink.
5. The flow is steady.
6. Radiation heat transfer is negligible.
7. The fluid is considered incompressible with constant properties.
8. Body forces are negligible.

Boundary conditions

The inlet (velocity inlet), outlet (pressure outlet), wall and symmetry boundary conditions were applied in the computational domain. The boundary conditions referring to Figure 4 are:

1. For the inlet section 1-8-16-9:

   $u(0,y,z)=u_{in}$, $v(0,y,z)=0$, $w(0,y,z)=0$ and $T(0,y,z)=T_{in}=293K$

2. For the bottom heated wall 2-3-6-7:

   $u(x,y,0)=v(x,y,0)=w(x,y,0)=0$ and $T(x,y,0)=T_w=343K$

3. For the section 1-4-5-8:

   $u(x,y,0)=v(x,y,0)=w(x,y,0)=0$ and $\left(\frac{\partial T}{\partial z}\right)_{x,y,0}=0$

4. The top wall 9-12-13-16 was considered to be adiabatic, where the no slip condition for the velocity components was applied:

   $u(x,y,z)=v(x,y,z)=w(x,y,z)=0$ and $\left(\frac{\partial T}{\partial z}\right)=0$

5. For sections 1-4-12-9 and 8-5-13-16, the symmetry boundary condition was applied (Sahiti *et al.* [13]) and in the outlet section 4-12-13-5, the pressure outlet boundary condition was used.

5. NUMERICAL SIMULATIONS

Computational code

The governing equations along with the boundary conditions were solved numerically by the finite volume method using commercial CFD software FLUENT 6.3. The second order upwind scheme was used to discretize the governing equations. The preprocessing tool GAMBIT was used for the creation of geometry and meshing. Dewan *et al.* [15] compared the numerical results with the experimental data reported in the literature for pin fin heat exchanger and a good agreement was obtained for RNG *k-ε* model with the standard wall function compared to that by other models. Hence for the present computation RNG *k-ε* model with standard wall function was used. The segregated solver was employed to obtain the numerical solution of the governing equations for the conservation of the mass, momentum, and energy and other scalar variables, such as turbulence. The SIMPLE algorithm was used to relate velocity and pressure corrections to enforce mass conservation and to obtain the pressure field. Sutherland's correlation was used for the variation of the molecular viscosity of air with temperature.

Computational mesh

The grid was generated using the commercial package GAMBIT 2.3.16. The unstructured meshes were used for all the geometries. The prismatic volume mesh was used for circular, elliptical, drop and hexagonal

geometries and tetrahedral volume meshes were used for 2º and 4º tapered circular pin fin geometries. A prismatic volume mesh was obtained from the triangular meshes with pave scheme on the surfaces and Hex/Wedge element with cooper scheme on the volume. Parts of the mesh used for elliptical pin fins heat exchanger are shown in Figure 6. A tetrahedral volume meshes was obtained from the triangular meshes with pave scheme on the surfaces and Tet/Hybrid element with TGrid scheme on the volume. A part of numerical mesh used for 2º tapered circular pin fins is shown in Figure 7.

The convergence criterion plays an important role in the numerical solutions therefore an appropriate convergence criterion must be selected so as to make sure that the solution is converged. In the present work two different convergence criteria of 10^{-4} and 10^{-6} were used and it was observed that the numerical values of the flow parameters taken at the two convergence criteria were almost identical. Therefore a convergence criterion of 10^{-4} was used for all subsequent computations. The solution was said to be converged only after all the residuals satisfied this criterion.

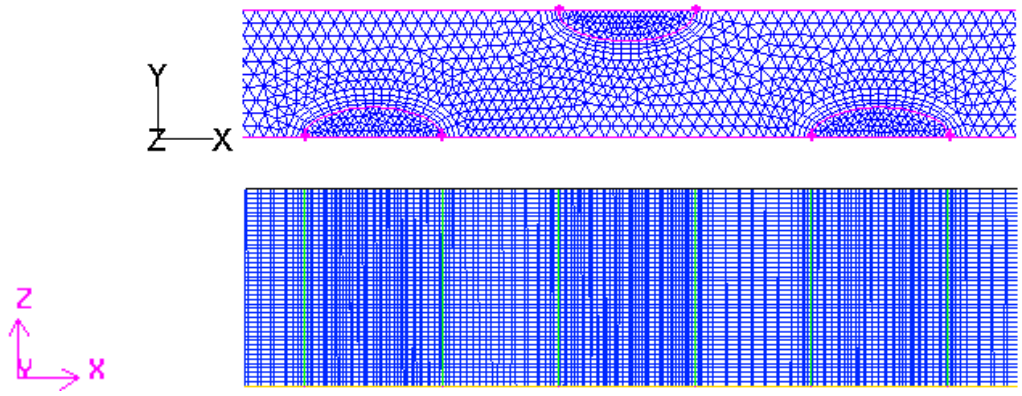

Fig.6. A part of numerical mesh used in elliptical pin fin arrangement.

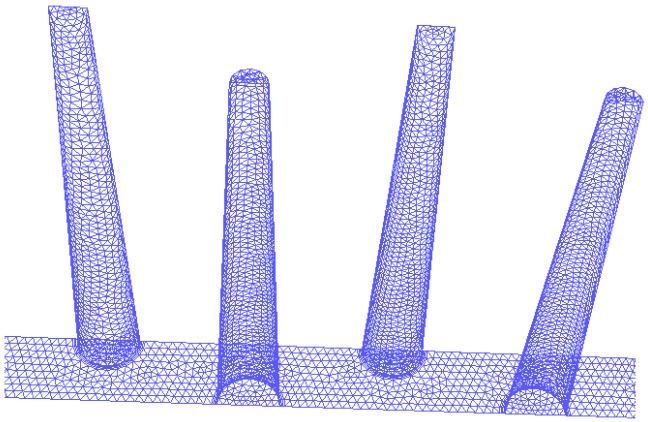

Fig.7. A part of numerical mesh used in 2^0 tapered circular pin fins arrangement.

Near wall treatment

Turbulence plays a dominant role in the transport of mean momentum and other parameters and therefore turbulence quantities should be accurately resolved. In the present work we have resolved, with sufficiently fine meshes, the regions where the mean flow changes rapidly and there are shear layers with a large mean rate of strain. Fine meshes were used in the vicinity of the fin surfaces to resolve the wall attached region. We can assess the near-wall mesh by displaying the values of non-dimensional distance from the wall $y^+ = \rho u_\tau y / \mu$ and Reynolds number Re. For the standard wall functions, each wall-adjacent cell's centroid should be located within the logarithmic layer, $30 < y^+ < 300$. However, a value of $y^+ = 30$ is the most desirable. A variation of y^+ for the wall adjacent cell centroid for the present computation showed that y^+ at the first node along the computational domain varies from 30 to 44 which means that the first grid points are located within the log layer.

Grid independence study

The grid independence study was performed for all six types of pin by using the RNG k-ϵ model with the standard wall functions for the inlet velocities ranging from 1.5 m/s to 6.0 m/s (Re = 205 to 820). Reynolds number is defined as $Re = (UD_h)/\nu$, where U, D_h and ν denote the inlet air velocity, hydraulic diameter and kinematic viscosity of air, respectively. In all cases, the mesh was very fine in the critical regions, i.e., in the vicinity of solid walls and both upstream and downstream of the pin fins. For the grid independence study (Table 1) four different types of mesh were selected according to the requirements of the geometries. The final selection of the mesh was based

on the least deviation between two successive mesh types. The details of the grid independence study are shown in Table 1 and Figure 8. Here MT-1 denotes mesh with 0.5 to 0.75 million elements, MT-2 with 0.75 to 1.05 million elements, MT-3 with 1.05 to 1.35 million elements and MT-4 with 1.35 to 1.65 million elements).

Table 1. Grid independence study.

Types of pin fins	Mesh types (MT)				Average % deviation in Nu values between			Selected Cells
	MT1	MT2	MT3	MT4	MT2 and MT1	MT3 and MT2	MT4 and MT3	
Elliptical	632544	918720	1103168	-----	1.10	0.13	------	918720
Straight circular	743498	913514	1100274	-----	5.29	0.41	------	913514
Drop	705726	907445	1236480	1585464	2.24	6.30	0.36	1236480
Hexagonal	578898	1018062	1335840	-----	2.45	0.36	------	1018062
2º Tapered circular	702418	953843	1108024	1436668	1.74	1.94	0.14	1108024
4º Tapered circular	697588	912648	1067252	1425784	3.68	1.36	0.785	1067252

Code validation

The validation of the present computational model was performed by comparing the present computations with the experimental data of Kays [1]. The present predictions by the RNG k-ε model using the standard wall function are in good agreement with the experimental data. An average deviation of approximately 20% between the two can be attributed to experimental uncertainties and limitation of modeling complex turbulent flow in this heat exchanger using the RANS equations (Figure 9). After having validated the code we proceed to perform comparisons of various pin fin cross-sections.

6. RESULTS AND DISCUSSION

The flow and heat transfer performances in compact heat exchangers surfaces mainly depend on the boundary-layer behavior over the interruptions, flow separation, recirculation, reattachment and vertices in the wake region. In Figure 10, the streamlines are drawn for all six types of pin fins for an inlet velocity of 5.0 m/s (Re = 685) on the x-y plane at z = 11.5 mm. The presented streamline encompass the flow after the fourth row of pin where the flow field is well developed. Streamline patterns around the pins clearly show that each pin is characterized by some back flow in the region behind the pin. The recirculation and boundary layer separation are smaller in case of elliptical and drop pin fins. This is because of streamline shape of both the pin fins, however in case of tapered circular, straight circular and hexagonal pin boundary-layers separate early and the wake behind the pin is large and wide. The Nusselt number and Colburn factor have rather large values in high Reynolds number region for drop and elliptical pin fins compared to straight circular pin fins. The point of separation in the former pin fins is possibly almost fixed over the range of Reynolds number considered in the present paper. However, for flow past a circular cylinder the point of separation depends on Re of incoming flow and therefore its thermal behaviour also depends on Re. A large amount of heat transfer at large Re for drop and elliptical pin fins compared to circular pin fin is probably due to a large separation region at high Re in case of former two fins compared to circular pin fin. However, at low Re the sizes of separation regions seem to be approximately the same for three pin fins (circular, drop and elliptical) resulting in similar values of Nusselt number and Colburn factor for these pin fins.

The temperature contours on the x-y and x-z planes along the streamwise direction are shown in Figure 11. It is seen that the fluid adjacent to the fins attains the maximum temperature. Heat is transferred from the bottom heated plate to the fins by conduction and from fins to the fluid by turbulent convection. The temperature difference between the fin and fluid decreases downstream along the computational domain. The fluid takes heat from the fins and hence the temperature of the fluid goes on increasing. The temperature difference between the fins and the surrounding fluid, which provides the temperature gradient, decreases along the length of the computational domain. The heat transfer rate and Nusselt number (Figures 12 and 13) of the fin increase with the Reynolds number. This is due to the fact that a higher fluid inlet velocity leads to larger convective heat transfer resulting in a larger increase of heat transfer rate with the increasing Re. The results indicate that the drop shaped pin fins yield a considerable improvement in the heat transfer compared to other pin fins for the same Reynolds number, however 4º tapered circular pin fins show minimum improvement in heat transfer rate. This improvement is mainly due to the increased wetted surface area of the drop pins, and the delay in the flow separation as it passes the more streamlined drop shaped pin fins.

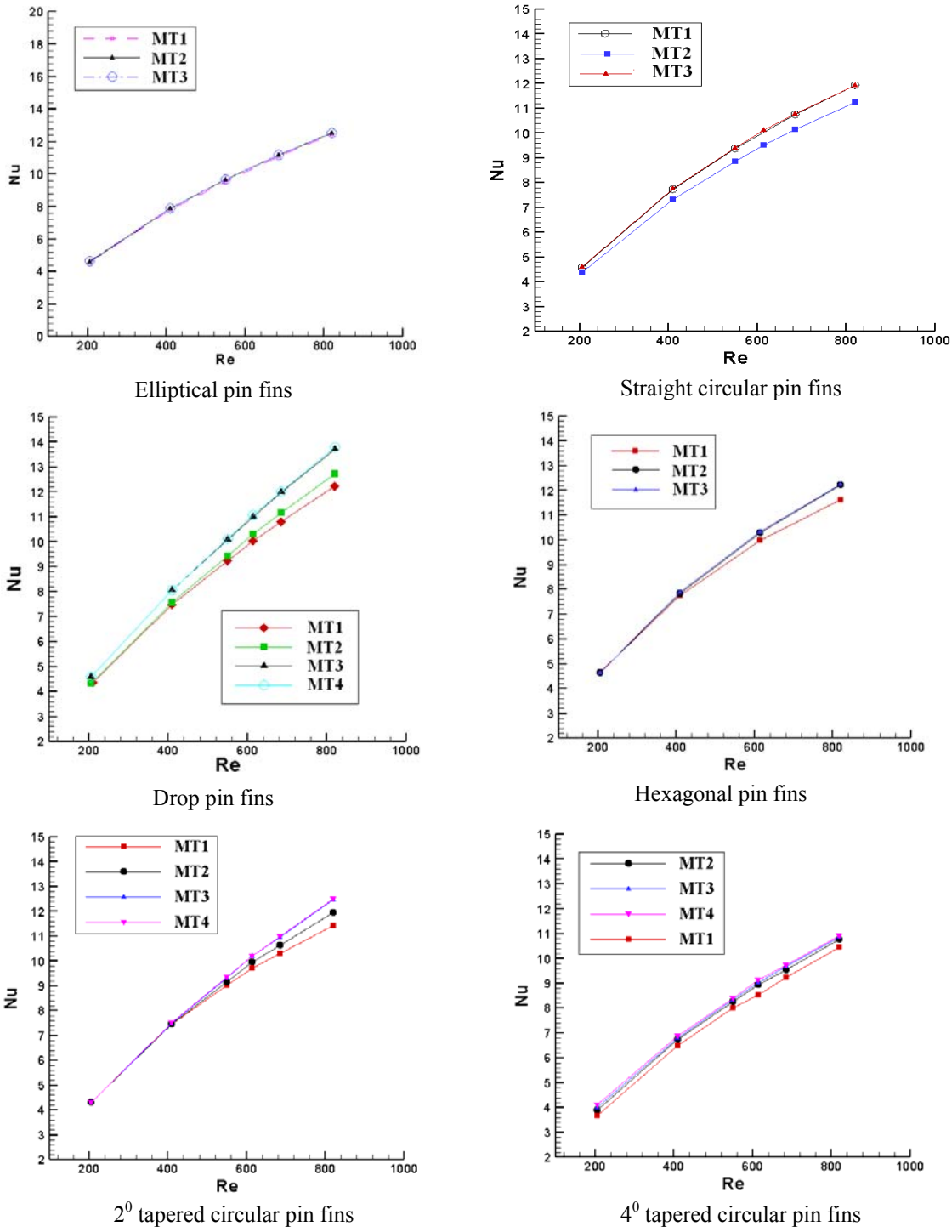

Fig. 8. Grid independence study.

Colburn factor (j) represents non-dimensional form of heat transfer and is given as $j = St\,\mathrm{Pr}^{2/3} = Nu/(\mathrm{Re}\,\mathrm{Pr}^{1/3})$. It is a standard practice in the literature to present this parameter as a function of Reynolds number. Figure 14 shows the Colburn factor variation with Reynolds number. A decrease in the Colburn factor is more for 4^0 tapered circular pin fin compared to others pin fin for the corresponding values of Re. However decrease in the Colburn factor for the same value of Re is minimum for drop pin fin, therefore heat transfer rates are higher for drop pin fins compared to that for circular pin fins.

Pressure drop plays an important role in the performance of pin fin heat exchanger. Therefore for the investigation of good pin fin we need to also focus on pressure variation in pin fin heat exchanger. Figure 15 shows a variation of static pressure along the streamwise direction. At the beginning of the pin array a pressure drop takes place as a consequence of the sudden flow contraction. Further downstream the flow path resembles a converging-diverging channel. Hence in each subsequent pin row a pressure loss due to the contraction and a pressure gain due to expansion of the flow occur.

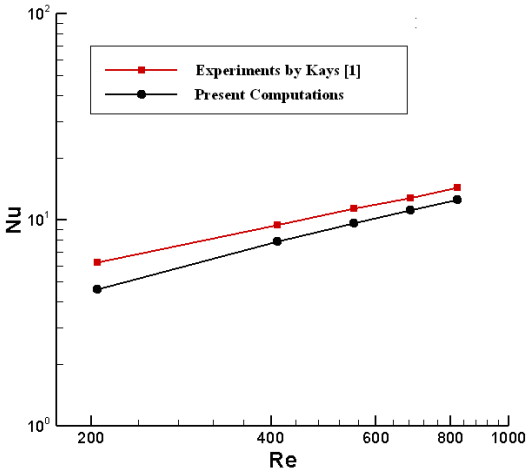

Fig. 9. Validation of the present numerical results of straight circular pin fins heat exchanger with experimental data by Kays [1].

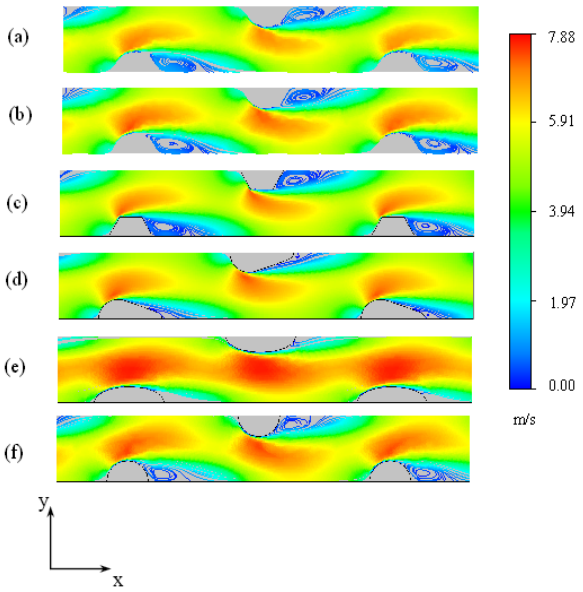

Fig. 10. Streamlines in the x-y plane at z = 11.5 mm, for inlet velocity 5.0 m/s (a) 4º tapered circular pin fin, (b) 2º tapered circular pin, (c) hexagonal pin fin, (d) drop pin fin, (e) elliptical pin fin and (f) straight circular pin fin.

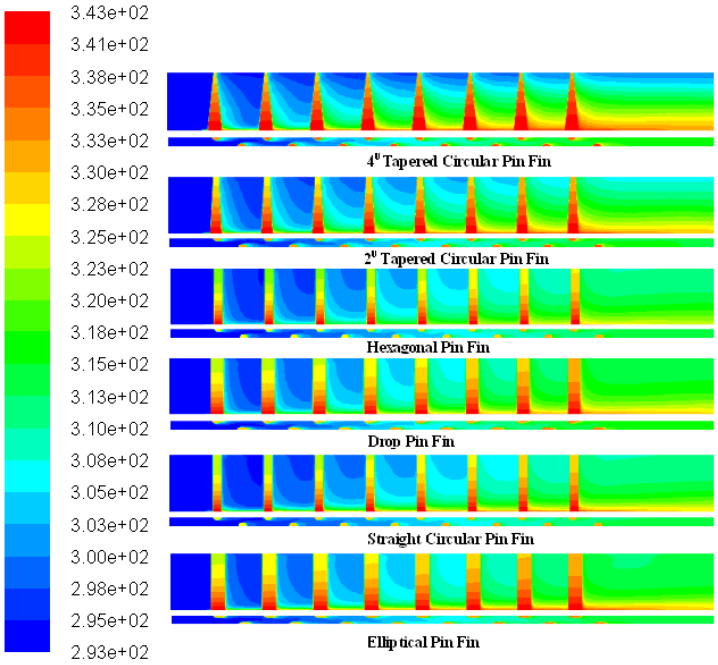

Fig. 11. Temperature contours along the streamwise direction for the inlet velocity of 5.0 m/s.

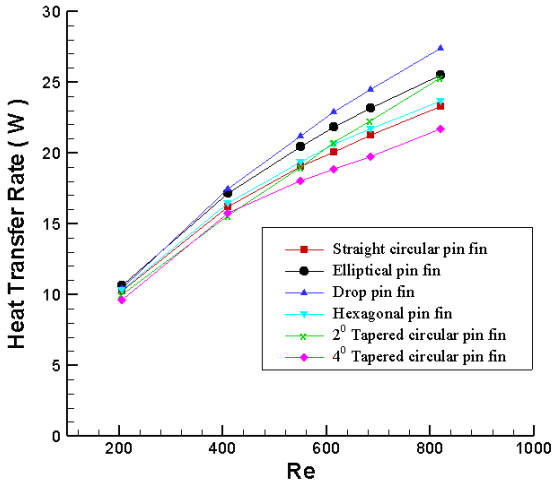

Fig. 12. Comparison of heat transfer rate variation with Reynolds number for different pin fin heat exchangers.

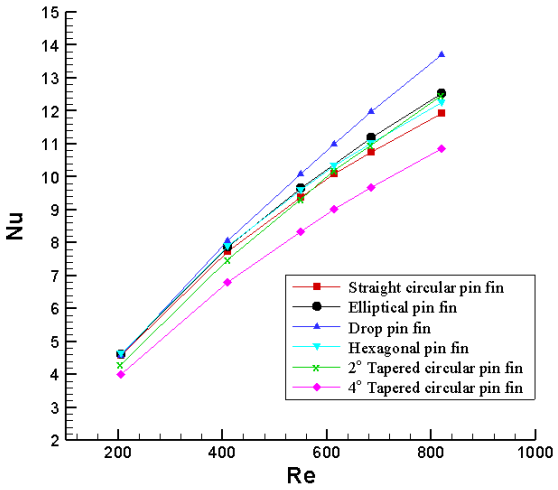

Fig. 13. Comparison of Nusselt number variation with Reynolds number for different pin fin heat exchangers.

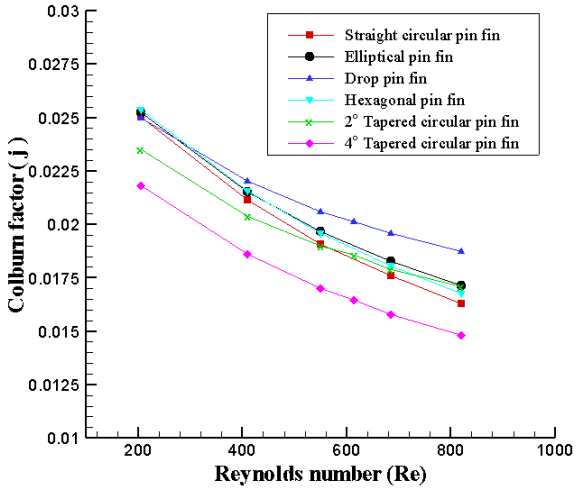

Fig. 14. Comparison of Colburn factor variation with Reynolds number for different pin fin heat exchangers.

The pressure drop can be calculated from the inlet and outlet pressure difference. As the inlet velocity increases the pressure drop also increases as shown in Figures 15 and 16. It can be noticed from Figure 15 the drop in pressure along the streamwise direction is higher for straight circular pin and minimum for elliptical pin fin. It can be clearly observed from Figures 15 and 16 that the degree of tapering significantly reduces the pressure drop compared to straight circular pin fin. Drop pin fin shows the second least pressure drop, because of the streamlined shape of drop pin fin. But the pressure drop also depends upon the skin drag and form drag. In case of drop pin fin form drag is significantly small compared to the skin drag. A streamline body experiences drag mainly due to the skin-friction at its surfaces, while a bluff body experiences smaller skin drag compared to the form drag resulting in high pressure drop in case of hexagonal pin fin compared to streamline shaped (i.e., elliptical and drop) bodies. Elliptical pin fin experience the least pressure drop because combined values of skin and form drags are small while in case of straight circular pin fin combined values of skin and form drags are larger.

A final assessment of the performance of the pin fin cross-section is based on the heat exchanger performance plot. Such a plot allows the assessment of the pin performance including their heat transfer and the pressure drop. It can be easily noticed from Figure 17 that the elliptical pin fin heat exchanger shows the highest heat transfer rate for the same pressure drop compared with other geometries.

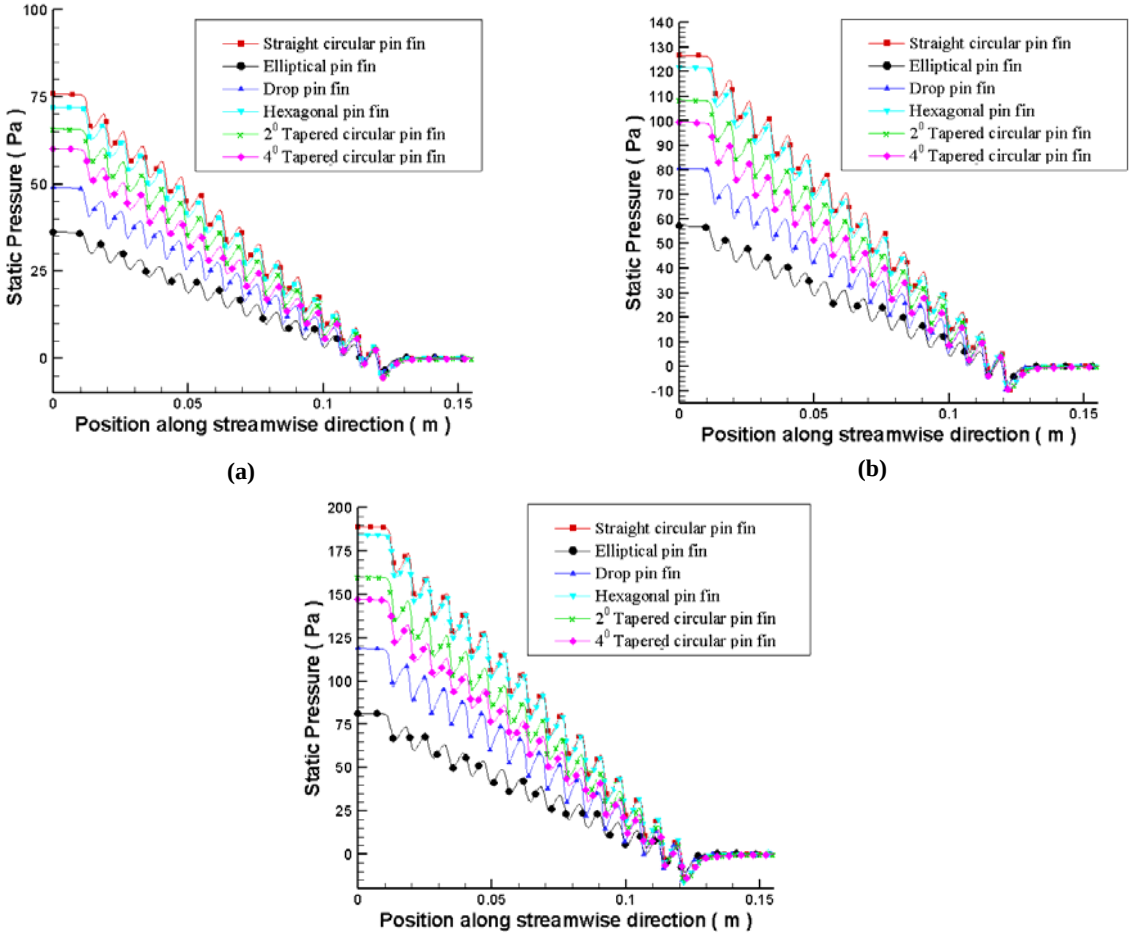

Fig. 15. Comparison of pressure variation for six types of pin fin heat exchangers along a line (i.e., x = 0 to 155.3, y = 1.8 mm, z = 11.5 mm) for (a) u = 3.0 m/s, (b) u = 4.0 m/s, (c) u = 5.0 m/s.

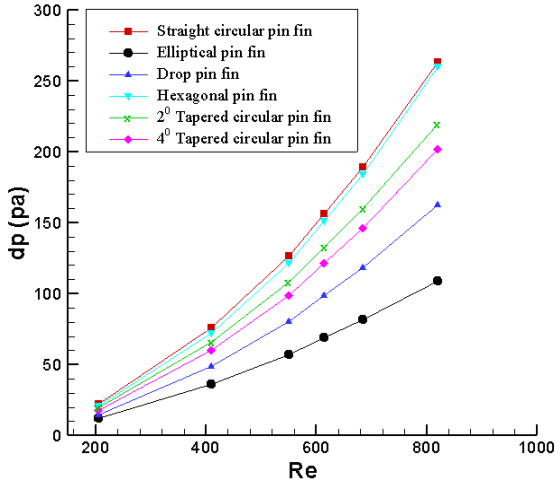

Fig. 16. Comparison of pressure drop with Reynolds number for six types of pin fin heat exchangers.

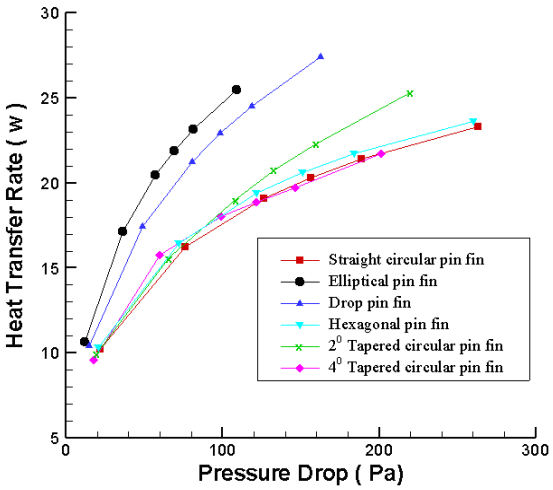

Fig. 17. Pin fin heat exchanger performance plot.

7. CONCLUSION

A comparative computational investigation of the thermo-fluid behaviors of six different types of pin fins heat exchangers has been presented using the RNG *k-ε* turbulence model with the standard wall functions. The aim of the present work was the comprehensive and systematic investigation of the influence of pin cross-section on the overall performance of the heat exchanger. The conclusions from the present study may be summarized as

1. The results of the simulation of six different pin cross-sections show that the elliptic profile performs better than all other pin cross-sections. This makes the elliptical fin arrays a promising device for the cooling of high thermal loaded electronic components.

2. By changing the pin shape from round to drop, there is an increase in the interaction between fin and fluid, which increases the total heat transfer rate. Drop pin experiences a somewhat higher pressure drop compared to elliptical pin fin heat exchanger at the same value of Re.
3. Degree of tapering has a significant influence on both fluid and thermal behaviors of pin fin. The 2^0 tapered circular pin fins performed better compared to 4^o tapered and straight circular pin fins.
4. The hexagonal profile which is similar to a bluff body does not show much advantage compared to drop, elliptic and 2^0 tapered pin fins. However its performance was somewhat better compared to 4^0 tapered and straight circular pin fins.

ACKNOWLEDGEMENT

The work reported here forms a part of the Department of Science and Technology, Government of India, New Delhi, sponsored project "Modeling and Computation of Three-Dimensional Turbulent Convective Heat Transfer for Design of Energy Efficient Pin Fin Heat Exchanger" (SR/S3/MERC-091/2007). A. Dewan and P. Mahanta gratefully acknowledge the financial support received from DST.

NOMENCLATURE

Cp	Specific heat at constant pressure
C_f	Friction coefficient
d	Diameter of fins
D_h	Hydraulic diameter
E	Enhancement ratio
H	Fin height
h	Heat transfer coefficient
J	Colburn factor

Greek Letters

ε	Dissipation rate
δ_{ij}	Kronecker delta
Δ	Drop
τ	Shear stress
μ	Dynamic viscosity
ρ	Density

Subscripts

k	Thermal conductivity
	Turbulent kinetic energy
L	Length
Nu	Nusselt number
P	Pressure
Pr	Prandtl number
Q	Heat flux
Re	Reynolds number = $(UD_h)/\nu$
S_D	Diagonal pitch
S_L	Longitudinal distance between two pin fins
S_T	Transverse distance between two pin fins
St	Stanton number
S	Longitudinal fin spacing
T	Temperature
U	Inlet air velocity
y^+	Nondimensional distance from wall
a	Air
f	Fluid
h	Hydraulic
w	Wall
t	Turbulent

REFERENCES

[1] Kays, W.M., 1955. Pin fin heat exchanger surfaces. *Transactions of. ASME* 77: 471- 483.

[2] Theoclitus, G., 1966. Heat-transfer and flow-friction characteristics on nine pin fin surfaces. *Journal of Heat Transfer* 383-390.

[3] Sparrow, E.M., Ramsey, J.W. and Altemani, C.A.C., 1980. Experiments on inline pin fin arrays and performance comparison with staggered arrangement. *ASME Journal of Heat Transfer*, 102: 44-50.

[4] Ota, T., Nishiyama, H. and Taoka, Y., 1984. Heat transfer and flow around an elliptical cylinder, *International Journal of Heat and Mass Transfer* 27(10): 1771- 1779.

[5] Lee, S., 1995. Optimum design and selection of heat sinks. In the Proceedings of *11th Annual IEEE Semiconductor Thermal Measurement and Management Symposium*, San Jose, California: 48-54.

[6] Babus'Haq, R.F., Akintunde, K. and Probert, S.D., 1995. Thermal performance of a pin-fin assembly. *International Journal of Heat and Fluid Flow* 16: 50-55.

[7] Chen, Z., Li, Q., Meier, D. and Warnecke, H.J., 1997. Convective heat transfer and pressure loss in rectangular ducts with drop-shaped pin fins. *Heat and Mass Transfer* 33: 219-224.

[8] Li, Q., Chen, Z., Flechtner, U. and Warnecke, H. J., 1998. Heat transfer and pressure drop characteristics in rectangular channels with elliptic pin fins. *International Journal of Heat and Fluid Flow* 19: 245-250.

[9] Behnia, M., Copeland, D. and Soodphakdee, D., 1998. A comparison of heat sink geometries for laminar forced convection, Numerical simulation of periodically developed flow inter society conference on thermal phenomena, pp. 310-315.

[10] Uzol, O. and C. Camci, 2001. Elliptical pin fins as an alternative to circular pin fins for gas turbine blade Cooling applications, Part 1: End wall heat transfer and total pressure loss characteristics, Pennsylvania State University, University Park, PA 16802.

[11] Moshfegh, B. and R. Nyiredy, 2004. Comparing RANS models for flow and thermal analysis of pin fin heat sinks, 15th Australian Fluid Mechanics Conference, Univ. Sydney, Sydney.

[12] Dewan, A., Mahanta, P., Raju, K.S. and Kumar, P.S., 2004. A review of passive heat transfer augmentation techniques, Proc. Inst. of Mechanical Engineers, Part A. *Journal of Power and Energy* 218: 509-527.

[13] Sahiti, N., Lemouedda, A., Stojkovic, D., Durst, F. and Franz, E., 2006. Performance comparison of pin fin in-duct flow arrays with various pin cross-sections. *Applied Thermal Engineering* 26: 1176-1192.

[14] Yang, K.S., Chu, W.H., Chen, I.Y. and Wang, C.C., 2007. A comparative study of the airside performance of heat sinks having pin fin configurations. *International Journal of Heat and Mass Transfer* 50(23-24): 4661-4667.

[15] Dewan, A., Dayanand, L. and Patro, P., 2008. Mathematical modeling and computation of three-dimensional, turbulent, convective heat transfer in a heat exchanger with circular pin fins. *App. Mathematical Modeling* (Ed. E.N. Virtanen), Nova Publishers, New York, USA, pp. 273-296.

[16] Yakhot, V. and S.A., Orszag, 1986. Renormalization group analysis of turbulence: I. Basic theory. *Journal of Scientific Computing* l(1): 1-51.

[17] FLUENT 6.3, Users Guide, Fluent Inc., Lebanon, USA.